Title
APPLICATION OF RATE THEORY TO DISLOCATION DYNAMICS

Authors
Dorn, John E.
Mukherjee, Amiya K.

Publication Date
1969-10-01

For AIME Symposium on Thermal and Non-Thermal Crystalline Deformation, Philadelphia, Pa., October 13-16, 1969

UCRL-19097
Preprint

c.2

APPLICATION OF RATE THEORY TO DISLOCATION DYNAMICS

John E. Dorn and Amiya K. Mukherjee

October 1969

AEC Contract No. W-7405-eng-48

LAWRENCE RADIATION LABORATORY
UNIVERSITY of CALIFORNIA BERKELEY

UCRL-19097

DISCLAIMER

APPLICATION OF RATE THEORY TO DISLOCATION DYNAMICS

Inorganic Materials Research Division, Lawrence Radiation Laboratory
Department of Materials Science and Engineering, and
College of Engineering University of California, Berkeley, California
John E. Dorn[1] and Amiya K. Mukherjee[2]

Abstract

This introductory report presents a brief survey of the current status of knowledge on the nature of the plastic behavior of metals and alloys. Major emphasis will be directed toward illustrating the progress that has been made in applying reaction-rate theory to describe thermally-activated motion of dislocations. In addition, an attempt will be made to identify those areas that are yet incompletely understood and require more detailed exploration.

[1]Professor of Materials Science, University of California, Berkeley and Senior Research Metallurgist, Inorganic Materials Research Division, Lawrence Radiation Laboratory, University of California.

[2]Associate Professor, Department of Mechanical Engineering, University of California, Davis, and Research Metallurgist, Inorganic Materials Research Division, Lawrence Radiation Laboratory, University of California, Berkeley.

I. Introduction

The plethora of "theories" on work hardening clearly exposes the confused state of knowledge on this topic. It is often thought that the subject of this report, namely thermally-activated dislocation dynamics, might be more firmly established, particularly in view of the more unified consensus on the operation of a number of such specific mechanisms. Upon deeper reflection, however, it becomes ever more evident that, despite preliminary experimental confirmation of some mechanisms, differences in opinion nevertheless persists on some details of thermally-activated deformation processes. The major problems concern the following: (1) Erecting a sufficiently accurate model for estimating the activation free energies for each type of obstacle. (2) Determining an appropriate kinetic framework for estimating frequencies of activation and the densities of mobile dislocations. (3) Ascertaining the origin and nature of the athermal stress level to permit evaluation of its influence on the mean dislocation velocity, and to permit selection of appropriate thermodynamic variables. (4) Introducing reasonably accurate dislocation-obstacle statistics, including effects of dislocation flexibility. (5) Undertaking the formidable task of accounting for the realistic condition of the simultaneous distribution of a number of different types of obstacles. (6) Erecting experimental approaches that provide checks on the internal consistency of the models.

It is the purpose of this report to outline briefly those facets of the subject that appear to be fairly well established, and to identify those aspects that are less well understood, and therefore, yet controversial. An attempt will be made to de-emphasize details of secondary importance so that major emphasis might be directed toward general issues of principles. It is not the purpose of this report to present a unified theoretical approach to the kinetics of dislocation mechanisms since this objective has not yet been achieved. However, those facets of the subject that must eventually be included in a comprehensive approach to kinetics of dislocation mechanisms will be described and discussed.

II. Classification of Deformation Mechanisms

For the purpose of this report deformation mechanisms might be grouped into four major classes (1). All mechanisms belonging to a given class have certain common features. Each individual class, however, exhibits uniquely different types of plastic behavior. Typical ranges of dominance for each class are illustrated by the τ-T-$\dot{\gamma}$ relationships obtained for single crystals of AgMg (2,3,4) as shown in Fig. 1. Yield point and dynamic strain-aging phenomena are absent in this example and will not be reviewed in this report. For the sake of brevity all symbols are defined in Appendix I.

In general, deformation at temperatures above about 0.45 T_m for low values of $\dot{\gamma}$ is determined by one or more of a series of diffusion-controlled mechanisms (5). The thermally-activated events in all such mechanisms are vacancy-atom exchanges in a stress-induced chemical-potential gradient of vacancies or solute atoms in the grain boundaries,

dislocation cores, or the volume of the crystal. In general, the steady-state rates are given by

$$\frac{\dot{\gamma}_s kT}{DGb} = A \left(\tau/G\right)^n \qquad (1)$$

where D is the appropriate diffusivity, and A and n are constants dependent on the mechanism and pertinent microstructural details. Since interest here centers about the distinctly different mechanisms of thermal activation of dislocations over barriers, no further reference will be made to diffusion-controlled mechanisms.

Over an intermediate range of temperatures the deformation is athermal and τ decreases very gradually with an increase in T, usually in a manner that parallels the effect of T on G. Athermal mechanisms fall into two major categories: those that are inherently athermal and those that are energetically athermal. An example of the former is given by the motion of a dislocation through a short-range ordered (6,7), or clustered alloy. In this example the energy of the system increases monotonically with the disordering across the slip plane as the area swept out by the dislocation increases. Since no maximum in energy is ever reached, such mechanisms are inherently athermal. In contrast, Frank-Read sources (8) are thermally activatable. Under a stress less than that required for immediate operation of the source, the dislocation segment bows out to a radius of curvature greater than one-half the segment length. A further virtual displacement of the dislocation results in an increase in the total energy since the increase in line energy at first exceeds the work gained due to the stress. As further virtual displacements are imposed on the segment the stress work begins to predominate and the energy reaches a maximum value. Consequently, Frank-Read sources are thermally activatable. A simple calculation, however, clearly reveals that the energy that need be supplied to operate such a Frank-Read source is so high that it seldom nucleates slip bands at temperatures below about $T_m/4$ unless the stress is almost equal to that needed to operate the source without the aid of thermal fluctuations. Similarly, the breaking of attractive junctions (9-11), bypassing of long dislocation segments, and the overcomming of long-range back stresses (12-14), although thermally activatable, are energetically athermal in the temperature range of interest here.

Disregarding statistical geometric details, the theoretical estimates for the athermal stress levels due to operation of Frank-Read sources, the breaking of attractive junctions, the bypassing of individual dislocations, and long range stress fields all give about the same answer, namely,

$$\tau_A = \beta Gb\sqrt{\rho} \qquad (2)$$

where $\underline{0.2} \leq \beta \leq \underline{0.5}$. Such nominal coincidence in τ_A for the various possible athermal mechanisms have contributed to the confusion regarding the origin and nature of strain-hardening. Both etch-pitting techniques and transmission electron microscopy, however, have confirmed the nominal validity of Eq. 2. In short- and long-range ordered alloys the athermal

stress levels are higher than those given by Eq. 1, as a result of the additive effects of disordering and production of antiphase boundaries. Typical examples are given by Ag_2Al (15) and AgMg (4). It will be shown later that the analysis of low-temperature thermally-activated mechanisms hinges sensitively on the origin of the athermal stress levels.

Our major interest centers about the low-temperature thermally-activated mechanisms over which the flow stress decreases precipitously with an increase in temperature. The many mechanisms that can be operative in this region are best grouped in two principal categories. One deals with localized barriers to the motion of dislocations such as forest dislocations (16), stress fields of solute atoms (17-22), semi-coherent precipitates (23), coherent precipitates (24,25), effects arising from radiation damage (26-28), etc. The other concerns nucleation of slip at linear barriers such as given by the Peierls (29-34), and pseudo-Peierls hills (35), Lomer-Cottrell locks (36), thermally activated cross slip (37-38) of dissociated screw dislocations, etc. Whereas, the two categories of barriers differ in kind of operative activation mechanisms, the details of the various mechanisms in each category differ only in degree. Furthermore, thermally-activated migration of dislocations past localized barriers is highly dependent on dislocation-localized barrier geometric statistics; in contrast, nucleation of slip past linear barriers is largely free from such auxiliary complications.

At $T = 0$, a stress τ_o (vide Fig. 1) is needed to push dislocations mechanically past all barriers. At $T>0$, however, thermal fluctuations can assist the stress in causing the dislocation to surmount barriers. Therefore, the value of τ needed to maintain a constant value of $\dot{\gamma}$ for a given substructural state decreases with increasing T due to the more energetic thermal fluctuations at higher temperatures. For the same τ, higher temperatures give higher frequencies of successful fluctuations and therefore, higher values of $\dot{\gamma}$. Above a temperature T_c, which increases with increasing $\dot{\gamma}$, thermal fluctuations are sufficiently energetic to cause dislocations to surmount all of the short-range barriers responsible for the low-temperature thermally activated mechanisms, even when the applied stress is only slightly above the athermal stress level. In some cases, e.g. when the Peierls and pseudo-Peierls mechanisms control the low-temperature thermally-activated deformation, there appears to be a more or less abrupt transition from the τ-T curve in the thermally activated region to the athermal τ-T curve in the athermal region. In other cases, e.g. when the low-temperature thermally-activated mechanisms controlled by cross-slip, overcomming solute-atom stress fields, or intersection of dislocations (particularly in low-stacking fault energy metals and alloys) the τ-T curve in the thermally activated region veers gradually and apparently asymptotically into that for the athermal region. In these instances the value of T_c cannot be accurately determined experimentally. This arises either when the activation energy increases rapidly as the applied stress is decreased so as to approach τ_A, or when the pre-Boltzmann term depends on the stress.

Stresses above τ_o (vide Fig. 1) can be applied by various impact

techniques. Such stresses are sufficiently high to force dislocations mechanically past all short- and long-range barriers to their motion. Due to their low inertia, dislocations subjected to such stresses accelerate rapidly and soon reach a limiting velocity which increases linearly with the net operative stress as determined by the sums of effects due to thermoelastic damping (39-41), flutter radiation of energy (42), electron viscosity (43,44), and phonon viscosity (45-48).

Damping mechanisms are of some interest to the present discussion because they are also operative in the thermally activated and athermal ranges of behavior. Once a barrier has been surmounted with the aid of a thermal fluctuation, the dislocation advances to the next barrier with an average velocity that approximates that dictated by damping mechanisms. Consequently, the total time for a thermally activated excursion is the time awaiting a successful fluctuation in energy plus the time of travel to the next barrier. Damping mechanisms also account for very slight increases in the measured stress with increasing strain rate in the athermal region. In addition, the stress in the "athermal region" may decrease slightly more rapidly than dictated by the change in modulus with increasing temperatures since most operative mechanisms are only energetically athermal and not inherently so.

As a result of the inherent versatility of dislocation reactions, a large number of dislocation mechanisms usually occur simultaneously. Occasionally one controls the deformation rate and thus becomes experimentally identifiable. Due to the unique differences between mechanisms, there is no single analytical approach to the analysis of data. In general identification of mechanisms must be based on correlations of the experimental data with predictions based on reliable models of possible mechanisms. It is indeed surprising, in view of the complexity of the problem, that substantial progress has been made in identifying some dislocation mechanisms. This achievement is especially remarkable since the operation of various mechanisms is seldom mutually exclusive and the macroscopic behavior often arises from a complicated interrelated confluence of a number of mechanisms.

All approaches to the formulation of the plastic behavior of materials are based on one or another of the two equivalent geometrically justified expressions, namely

$$\dot{\gamma} = \rho_m b v = NAb \nu_A \qquad (3)$$

The effect of τ, T and substructure on ρ_m and v or on N, A, and ν_A is deduced from the model. Unfortunately the deduced dependency of $\dot{\gamma}$ on τ, T, and the substructure is often sensitive to the factors that were considered in erecting the model. These issues will now be illustrated in terms of selected models for cutting localized obstacles.

III. Activation Energies

A factor of major consequence in establishing v or ν_A is the activation free energy. Once a model is clearly visualized it is possible to estimate the activation free energy. Consider, for example,

the simple case illustrated in Fig. 2 of dislocations being thermally activated over a square array of rigid localized repulsive barriers characterized by a rectangular force-displacement diagram. The extra energy needed to mechanically and reversibly push the dislocation in the forward direction over the barrier under constant T and τ^* is given by $\alpha \Gamma b - \tau^* b^2 l_s$. For the present it will be assumed that $\nu+ = \nu^1 \exp - (\alpha \Gamma b - \tau^* b^2 l_s)/kT$ is valid where ν^1 is the attempt frequency. The evaluation of ν^1 and the justification for utilizing $\exp - (\alpha \Gamma b - \tau^* b^2 l_s)/kT$ for the probability of obtaining a successful fluctuation will be discussed in a later section. The net frequency of the forward reaction is given by

$$\nu_A = \nu^1 \left\{ e^{-\left(\frac{\alpha\Gamma b - \tau^* b^2 l_s}{kT}\right)} - e^{-\left(\frac{\alpha\Gamma b + \tau^* b l_s^2}{kT}\right)} \right\} \tag{8}$$

and therefore

$$\dot{\gamma} = \left(\frac{\rho_m}{l_s}\right) l_s^2 b \nu_A = \rho_m l_s b \nu^1 e^{-\left(\frac{\alpha\Gamma b - \tau^* b^2 l_s}{kT}\right)} \left\{ 1 - e^{\frac{-\tau^* b l_s (l_s + b)}{kT}} \right\}$$

When $\tau^* b l_s (b+l_s) \gg kT$, the last term of Eq. 4 becomes negligible and the common formulation omitting this term is obtained. On this basis the τ^*-T relationship is that given by the broken lines of Fig. 3 where T_c increases with $\dot{\gamma}$ according to

$$\alpha \Gamma b = kT_c \ln \frac{\rho_m l_s b \nu^1}{\dot{\gamma}} \tag{9}$$

At low values of τ^* the reverse reaction becomes significant and for the case where $l_s = 100$ b, the complete analysis give the solid curves of Fig. 3, showing that τ^* decreases asymptotically to zero as T increases. In general neglecting the back reaction for cutting localized barriers does not materially affect the shape of the τ^*-T curve except at very low values of τ^*. However, as will be described later, neglect of the reverse reaction in the Peierls mechanism for pinned dislocations can lead to serious error in analysis.

The force-displacement diagram of Fig. 2 is approximated only for the special case of intersection of repulsive trees during basal glide of undissociated dislocations in hexagonal crystals. More complicated diagrams apply for all other localized barriers. For example, when the glide dislocations are dissociated so that the equilibrium separation of the partial dislocation is about 5b, the force-displacement diagram is approximated by that given in Fig. 4b. Here the barrier force first increases with displacement due to constriction of the partial dislocations and the rectangular section from χ = 5 to 6 b is taken to be due to jog formation. For this example the τ^*-T relationship is that given in Fig. 4c. These examples reveal that the τ^*-T relationships depend sensitively on the shape of the force-displacement diagrams.

IV. Effect of Distribution of Obstacles

The simplifying assumption that localized obstacles form a regular square array is never valid. In cold-worked metals the dislocations are primarily concentrated in the entanglements comprising the cell walls. Up to the present no serious attempt has been made to take such geometrical distribution of obstacles into account in any model for thermally-activated intersection of repulsive trees. Theoretical analyses by Kochs (49), and extensions by others (50), have shown that the flow stress at the absolute zero is significantly different for random distributions of obstacles than that given for regular square arrays. This has been confirmed by the computerized experiments of Foreman and Makin (51). Friedel's (52) theory for the steady-state thermally-activated motion of dislocations past weak obstacles gives a close approximation of the statistical correction.

As shown in Fig. 5 a successful thermal fluctuation at B causes the dislocation to move forward. At the steady state it will just contact new obstacles at B'. On the average the area swept out per activation is given by $lh' = l_s^2$, the average area per obstacle. Furthermore, l and h' are related geometrically by $l^2 = R^2 - (R-h')^2 = 2Rh' - h'^2$. For weak obstacles $h' \ll 2R$ and $l^2 \simeq 2Rl_s^2/l$. Since

$$l \simeq \left(2 R l_s^2\right)^{1/3} = \left(2 \frac{\Gamma}{\tau^* b} l_s^2\right)^{1/3} \qquad (10)$$

the isothermal stress work done during thermal activation is $\tau^* b^2 l = 2^{1/3} \Gamma b (\tau^* l_s b/\Gamma)^{2/3}$. It is significant to note here that $l \equiv l\{\tau^* T\}$ where its dependence on T occurs via the shear modulus of elasticity, since $\Gamma \simeq Gb^2/2$. The mean dislocation velocity is

$$v = h' \nu^1 e^{-\frac{l}{kT}} [\alpha\Gamma b - \tau^* b^2 l] \left\{1 - e^{-\frac{l}{kT}(\tau^* b l_s^2 + \tau^* b^2 l)}\right\}$$

which reduces to

$$v = l_s^2 \left(\frac{\tau^* b}{2\Gamma l_s^2}\right)^{1/3} \nu^1 e^{-\frac{l}{kT}\left[\alpha\Gamma b - \Gamma b 2^{1/3} \frac{\tau^* l_s b}{\Gamma}^{2/3}\right]} \left\{1 - e^{\frac{l}{kT}\left[\tau^* b l_s^2 + \Gamma b 2^{1/3}\right]\left(\frac{\tau^* l_s b}{\Gamma}\right)^{2/3}}\right\} \qquad (11)$$

when the values of h' and l are introduced. A comparison of the τ^*-T relationship deduced from $\dot{\gamma} = \rho_m bv$ for the square array of obstacles and for a random arrangement to which Friedel's steady-state correction has been applied is shown in Fig. 6. Obviously the τ^*-T is highly sensitive to the distribution of obstacles.

V. Elastic Strain Centers

An extensive literature has been developed that proposes to describe the deformation characteristics due to thermally-activated motion of dislocations past localized stress fields arising from the presence of

substitutional and interstitial solute atoms (17-22), semi-coherency strains, tetragonal point defects (19-22), and centers of radiation damage (26-28). The importance of this subject demands at least a qualitative discussion of the various difficulties that are encountered in establishing reasonably realistic models for such processes: (1) Interaction energies are maximum for configurations where dislocation cores overlap the strain centers. Consequently, force-displacement diagrams are not well-known for the most significant configurations where the highest forces are encountered. (2) On the slip plane near most interesting strain centers, the local strains are so high as to invalidate the commonly adopted linear theory of elasticity. As a result of issues 1 and 2, the estimated values of τ^* are frequently seriously in error in the low-temperature range where τ^* is highest. (3) The often adopted simplifying assumption that only those strain centers which yield the highest localized stresses, namely those on atomic planes immediately above and below the slip plane, need be considered is not wholly justified even at low temperatures where τ^* has its highest values. For higher temperatures, where τ^* approaches zero, this simplifying assumption is patently invalid. (4) Interaction energies are usually highly sensitive to orientations of the dislocation and the defect. Consequently, the barriers to dislocation motion are characterized by a series of different activation energies. (5) In most approaches no consideration is given to the fact that the strain centers are usually more or less randomly distributed. As shown in the preceeding section this neglect can result in serious inaccuracies. (6) Equal numbers of attractive and repulsive strain centers are present. At low concentrations of such strain centers dislocations meander between the attractive and repulsive regions so as to minimize their energy. At higher concentrations, however, dislocations assume positions nearer those at the top of the stress barriers because of their limited flexibility. Although the general importance of dislocation flexibility had been recognized for sometime (53-55), it is only recently that semi-quantitative probes into the effect of flexibility have been made relative to the athermal deformation behavior at the absolute zero (50,56,57). Although these analyses need much refining there is no question concerning the fact that the effects of dislocation flexibility can be large. Furthermore, the usual prediction for atomic strain center models that $\tau^* \propto \sqrt{c}$ where c is the solute atom concentration, is shown to become invalid as c increases. No adequate analysis of the role of flexibility has yet been made for thermally activated cutting of stress fields arising from strain centers. (7) Several additional admitted crudities of analyses have also been made on second order issues which will not be reviewed here.

It now appears that no wholly satisfactory realistic models for thermal activation of dislocation past localized strain centers are currently available. This statement applies *a fortiori* to the complicated situations encountered as a result of radiation damage. Current statistical models (1,58,59) on deformation of radiation damaged alloys are illustrative of the inherent complexity of the problem.

Experimentally estimated force-displacement diagrams (60,61) for substitutional solid solution alloys are often found to be about the

same as those for the pure host metals. In these instances the major effect of alloying appears to be attributable merely to an increase in the dislocation density. In other examples experimentally deduced force-displacement diagrams change upon alloying probably as a result of changes in their stacking fault energies.

VI. Long-Range Internal Stress Fields

In this section a brief discussion will be presented on the effects of long-range internal stress fields on the macroscopic plastic deformation in the low-temperature thermally-activated range. Such long-range internal stress fields will be assumed to exist and for the present the influence of all other pertinent athermal mechanisms will be neglected. The effects of auxiliary athermal mechanisms on the plastic behavior in the thermally-activated region will be discussed later.

In general the details of the magnitude and distribution of internal stresses are not well known except for the fact that $\int \tau_i dxdy$ over the X-Y slip plane is zero. The qualitative effects of internal stress fields on the thermally activated behavior, however, might be estimated by representing the internal back stresses by a step function of amplitude τ_A' and wave length λ along the slip direction X, where $\tau_i = \tau_A'$ for $0 \leq x \leq \lambda/2$ and $\tau_i = -\tau_A'$ for $\lambda/2 \leq x \leq \lambda$. In the absence of other contributions to the athermal stress level, τ_A' can be associated with the previously discussed value of τ_A. For simplicity all localized obstacles will be assumed to have rectangular repulsive force-displacement diagrams as shown in Fig. 2. The back forces acting on a dislocation are the sums of those due to long-range back stresses and those arising from the local obstacles as depicted schematically in Fig. 7. The contacting segment length l of the dislocation is taken to be that given by the Friedel steady-state analysis. The active force on each obstacle due to the applied stress, τ, is shown by the broken line. Consequently, the energy that must be supplied by a thermal fluctuation to cut the localized barriers is given by the area of each localized barrier above the broken line. It is now evident that, despite the assumption that all isolated barriers had equal heights, the presence of long-range internal back stresses in general introduces a spatial distribution of a range of activation energies.

For the simple example that was selected for illustration, the activation energies for the forward reaction are shown in Table I. The net average dislocation velocity over the entire interval of $0 \leq x \leq \lambda$ is simply

$$\bar{v} = \frac{\lambda}{t_{o-\lambda/2} + t_{\frac{\lambda}{2}-\lambda} + t_D} \qquad (12)$$

where $t_{x_1-x_2}$ are the average rest times per thermal activation and $t_D \simeq \lambda/v_D$ where v_D is the average velocity of the dislocation as dictated by the operative damping mechanisms. Usually t_D is small relative to the net rest times per thermal activation. Under these conditions

$$\bar{v} = \frac{\lambda}{\frac{\lambda}{2\nu_{0-\lambda/2}} + \frac{\lambda}{2\nu_{\lambda/2-\lambda}}} = \frac{2}{\frac{1}{\nu_{0-\lambda/2}} + \frac{1}{\nu_{\lambda/2-\lambda}}} \qquad (13)$$

where the subscripts refer to the x ranges for each mean value of velocity. These values of ν are given by Eq. 11 upon replacing τ^* by $\tau-\tau_A'$.

Thus when $0 \leq \tau\, b^2 l \leq \tau_A'\, b^2 l$ the dislocation velocity is zero because ν^+ is zero for the region where $0 \leq x \leq \lambda/2$. For conditions II and III*, a somewhat higher value of $\dot{\gamma}$ is obtained for the same value of τ^* when the variations in the long-range stress fields are taken into account. The simple distribution of long-range internal stresses assumed here the maximum effect occurs for condition III where $\nu_{\lambda/2-\lambda}$ is effectively infinite and therefore $\nu = 2\nu_{0-\lambda/2}$. This amounts to doubling the value of $\dot{\gamma}$ for fixed values of T and τ^*. Alternately for constant values of $\dot{\gamma}$ and T, a very small and often negligible decrease in τ^* results. More realistic distributions of internal stress fields will give about the same results.

The above conclusions differ from those presented by previous investigators (62-64). This difference is due to the assumption made here, which was not invoked in previous analyses, that the local barrier forces are superimposed on the long-range back forces.

VI. Other Possible Sources of Athermal Stress

The principle of superposition is applicable when the athermal stress level arises exclusively from long-range internal stress fields. It also applies to the athermal stress, τ_s, arising from the disordering of short-range ordered alloys across the area swept out by dislocations. When both effects are present simultaneously the total athermal stress level is given by the sums of each individual contribution.

When superposition applies the analyses of experimental data are much facilitated. The athermal stress level can be extrapolated into the thermally activated region as shown by the broken line in Fig. 8, where the slope of the line parallels that for the effect of temperature on the shear modulus of elasticity. The effective stress τ^* for a given $\dot{\gamma}$ is then superimposed on the athermal stress level as shown in Fig. 8, giving the τ-T relationship represented by curve (a). When strain-hardening merely increases the superimposable athermal stress level without influencing the nature and distribution of the short-range barriers, and other factors are the same, the τ-T relationship shown in curve (b) is obtained within the accuracy suggested in the preceeding section. Consequently almost identical τ^*-T curves are obtained for wide ranges of values of superimposable τ_A where $\tau^*=\tau-\tau_A$.

The relationship illustrated in Fig. 8 is not always valid, however. In fcc metals over Stages I and II the athermal stress level increases in proportion to the density of the short-range barriers. Then a

*See Table I

substantially constant Cottrell-Stokes (65) ratio is obtained in Fig. 9.

It has been common practice in analysis of experimental data to invoke the concept of superposition without regard to the source of the athermal stress. The principle, however, is not universally valid. For example, there is no established theoretical justification for applying this principle to cases where the athermal stress might arise exclusively from that needed to operate Frank-Read sources or that needed to break attractive junctions. If, however, the long-range internal stresses are greater than those needed to operate Frank-Read sources or break attractive junctions, they will control and the previously discussed superposition principle will apply. The operative Frank-Read sources and attractive junctions will be those in the regions where the internal stresses are in the same direction as the applied stress.

The principle of superposition, however, is definitely invalid for the interesting example presented recently by Ono and Sommer (66). Only a brief outline of their analyses can be presented here. They considered the Peierls mechanism based on the nucleation of double kinks in segments of length 2L strongly pinned at their extremities by solute atoms. Thus $2L = b/2c$ where c is the atomic fraction of the solute atoms. In the absence of other sources of athermal stresses they demonstrated that the thermal energy, U_n, required to nucleate a pair of kinks, increased with decreasing values of τ/τ_p and decreasing values of L/b as shown by the solid lines in Fig. 10. After the pinned segment had advanced one Burgers' vector it had an activation energy U_{nb} nucleating a pair of kinks in the reverse direction as shown by the broken curves of the figure. The values of U_{nb} increase with increasing stress τ/τ_p and decreasing values of L/b as shown by the dotted lines of Fig. 10. The parametric solution where $U_n = U_{nb}$ for the same values of τ/τ_p gives the dashed curve marked L_c. As a result of the equality of activation free energies for the forward and reversed reactions, L_c demarks critical segment lengths below which dislocations cannot move and above which they can move forward. Fig. 11 gives the approximate relationship that $\tau_c/\tau_p \simeq 10b/L = 40c$. Thus τ_c is a lower cut-off stress, proportional to τ_p, which must be exceeded in order to induce plastic flow. When τ/τ_p exceeds that for τ_c/τ_p for a given L/b, the activation energy for the reverse reaction becomes much higher than that for the forward reaction and approaches that for $L = \infty$. Thus, as shown in Fig. 12, τ/τ_p versus $U_n/2U_k \simeq T/T_c$ reduces to the Dorn-Rajnak relationship for $L = \infty$ for high values ot τ/τ_p. The athermal stress, due to solute atom pinning effects, truncates the lower part of the diagram and the principle of superposition is not applicable in this example. The theory appears to be in fair agreement with the data of Nakada and Keh (67) on the effect of nitrogen on the low temperature plastic deformation of Fe where athermal stresses due to other causes seemed to be small. The theory however, is seriously incomplete inasmuch as interactions between the advancing dislocation line and strain centers of solute atoms was neglected.

VIII. Transition-State Reaction-Rate Kinetics

In the preceeding discussion the frequency of a thermally activated event was assumed to be given by

$$\nu+ = \nu^1_e \, {}^{-U}/_{kT} \tag{14}$$

The justification for this formulation and the physical identity of ν^1 will be presented here in terms of transition-state kinetics which is best exemplified by Eyring's reaction rate theory (68). Since the activation of a dislocation over a local barrier involves principally shear straining, the analysis will be based on a constant volume system.

A major assumption of the transition-state theory is that a thermodynamically well-defined transition state exists at the saddle point region of the potential energy surface. In the simplest case of the motion of a single atom over a barrier, the transition state is characterized by one degree of translational freedom along the reaction coordinate, χ_1, and two degrees of vibrational freedom in a plane, $\chi_2\chi_3$ normal to the reaction coordinate. To simplify the formulation the hypothetical case will first be assumed where interaction energy between the moving atom and the surrounding atoms are neglected. Over a small region δ along the reaction coordinate the potential energy is ε^* above the original vibrational ground states and the atom has mean translational velocity $\bar{v}'$. Consequently, the frequency of activation per atom in the initial state is given by

$$\nu^+ = \frac{N_a^*}{N_a} \frac{\bar{v}'}{\delta} = \frac{N_a^*}{N_a} \left(\frac{kT}{2\pi_m}\right)^{1/2} \frac{1}{\delta} = \frac{Z^*}{Z} e^{\frac{-\varepsilon^*}{kT}} \left(\frac{kT}{2\pi_m}\right)^{1/2} \frac{1}{\delta} \tag{15}$$

where N_a^*/N_a is the equilibrium number of atoms in the activated state per atom in the initial state. The partition functions, Z* and Z, for the activated and initial states are evaluated from their individual ground state values. Since only one atom is considered to be involved

$$Z^* = Z_{1t}^* \, Z_{2v}^* \, Z_{3v}^* = (2\pi mkT)^{1/2} \frac{\delta}{h} \, Z_{2v}^* . Z_{3v}^* \tag{16a}$$

$$Z = Z_{1v} . \, Z_{2v} . \, Z_{3v} = \frac{1}{1-e^{\frac{-hv_1}{kT}}} \, Z_{2v} . \, Z_{3v} \tag{16b}$$

where the subsctipts t and v refer to translational and vibrational states. Therefore,

$$\nu^+ = \frac{kT}{h} \left(1-e^{\frac{-hv_1}{kT}}\right) \frac{Z_{2v}^* \cdot Z_{3v}^*}{Z_{2v} \cdot Z_{3v}} e^{\frac{-\varepsilon^*}{kT}} = \frac{hT}{h} \left(1-e^{\frac{-hv_1}{kT}}\right) e^{\frac{-f^*}{kT}} \tag{17}$$

where f* is the Helmholtz free energy of activation.

Extrapolation of Eq. 17 for thermally activated motion of dislocations over localized barriers is beset by two major types of

difficulties. The first is due to the fact that many elastically coupled atoms participate in the thermally activated event and the second arises becauses no simple and analytically facile atomistic model for a dislocation has yet been erected to deal with activation events. For the present, however, the free energy of activation, f*, might be approximated by a hybrid model which involves the continuum string concepts where this is most useful, plus features ascribed to atomistic concepts where this appears to be fruitful. The isothermal shear work of activation, U, constitutes a major part of f* (33,69). It is a Helmholtz free energy of activation and not, as was often assumed in the early literature on this subject, an activation energy. It contains both energy and entropy terms. U is calculated in terms of a static string model of a dislocation, and therefore, does not explicitly include energies and entropies of vibration. In the absence of a simple dynamical approach it appears suitable to neglect the elastic coupling between the atoms and assume that the activated event also involves m, Einstein linear harmonic oscillators (70). The number of oscillators m, involves only those atoms in the proximity of the localized barrier whose frequencies of vibration might be altered during the activation event. On the basis of this approximation

$$f^* \simeq U - kT \ln \frac{Z_2^*, Z_3^* \ldots Z_{m+1}^*}{Z_2, Z_3 \ldots Z_{m+1}} \qquad (18)$$

where now each vibrational partition function must include its ground state energy, namely,

$$Z_i = \left(2 \sinh \frac{h\nu_i}{2kT}\right)^{-1} \qquad (19)$$

assuming that the change in vibrational energy was not appropriately accounted for in the line energy estimate of U. According to the above approximations, the frequency of activation is given by the three equivalent expressions

$$\nu^+ = \nu'_1 \, e^{-U/kT} = \frac{kT}{h}\left(1-e^{\frac{-h\nu_1}{kT}}\right) e^{\frac{-f^*}{kT}}$$

$$= \frac{kT}{h}\left\{1-e^{\frac{-h\nu_1}{kT}}\right\}\left\{\prod_{i=2}^{m+1} \frac{\sinh \frac{h\nu_i}{2kT}}{\frac{h\nu_i^*}{2kT}}\right\} e^{-U/kT} \qquad (20)$$

Whereas it is customary in analyses of data on dislocation kinetics to assume that the frequency term $kT\,(1-e^{-h\nu_1/kT})/h$ is constant, the preceeding formulation suggests that it decreases with decreasing temperatures. For very low temperatures where $h\nu_1/kT$ is greater than about 3 the value of $kT(1-e^{-h\nu_1/kT})/h$ reduces to kT/h as suggested by Eyring (68). For high temperatures, however, where $h\nu_1/kT \ll 1$, it reduces to ν_1 as suggested by Wert and Zener (71).

The frequency term ν^1 is also dependent on the temperature. At high temperatures it reduces to

$$\nu^1 = \frac{\nu_1 \cdot \nu_2 \nu_3 \cdot\cdot \nu_{n+1}}{\nu_2^* \cdot \nu_3^* \cdot\cdot \nu_{n+1}^*} \tag{21}$$

which is analogous to the frequency term for atomic jumps in diffusion deduced by Vineyard (72) on the basis of classical statistical mechanics and similar to that for activation of solute-atom pinned dislocations given by Granato, Lucke, Schliff and Teutonico (73), who also used classical statistical mechanics.

It is interesting to note that whereas the various atomic frequencies for the activated state are undoubtedly constants as determined by the dislocation-barrier configuration at the saddle point energy, the frequencies of the atoms in the initial state are not constants. As the stress τ^* is increased the interaction energy between atoms in the near vicinity of the dislocation and the localized barrier increases and therefore, $\nu_i \equiv \nu_i \{\tau^*\}$. Thus, as the effective stress is increased the term

$$\left\{ \prod_{i=2}^{m+1} \frac{\sinh h\nu_{i/2kT}}{\sinh h\nu^*_{i/2kT}} \right\}$$

of Eq. 20 approaches unity.

The frequency ν^1 is often equated with the first mode of vibration of the dislocation line treated as a vibrating string. According to the Friedel approximation $\nu^1 \simeq \nu_o\, b/l$ where ν_o is the Debye frequency and l is the free length of the dislocation segment. This suggestion, based principally on intuition, yet requires definitive confirmation. For example, confluence of phonon interactions with smaller segments of the dislocation particularly in the vicinity of the barrier, might induce shock waves of sufficient intensity to facilitate thermal activation. Much need yet be done to provide a satisfactory estimate of ν^1.

Eq. 20 provides an internally consistent formulation of the thermodynamics for thermally-activated rate kinetics. All of the thermodynamic quantities such as the energy, entropy, and area of activation can be deduced directly from this expression. Furthermore, since the change in the shear modulus of elasticity with temperature reduces to zero at the absolute zero of temperature, the entropy of activation is also zero at 0°K. Thus the formulation presented here is completely consistent with the detailed thermodynamic approach presented by Li (74).

IX. Thermodynamical Variables

In the earlier sections of this survey it was assumed that the isothermal work of activation could be represented as $U \equiv U\{\tau^*, T\}$. This viewpoint has been adopted by a number of investigators. More recently other investigators (69,75,76) have argued that such a formulation is not thermodynamically acceptable and that U must be couched as $U \equiv U\{\tau, T\}$. Supporting arguments for the latter viewpoint are as follows:

1. Thermodynamic considerations must apply to the whole system and not simply those regions where the internal back stresses are a maximum.

2. The motion of a dislocation during the activation event induces shear displacements throughout the lattice.

3. These remarks suggest that the variables τ and T (not τ^* and T) remain constant during the activation event and should therefore serve as the appropriate thermodynamic variables.

Section VIII of this report, however is applicable in either case, since the appropriate variables for U were not specified.

Hirth and Nix (70) have recently criticized the validity of these arguments, suggesting that $U \equiv U\{\tau^*, T\}$ provides an equally correct selection of independent thermodynamic variables within the context of the auxiliary assumptions common to both formulations. A detailed comparison of the two approaches given in their report will not be reproduced here.

1. Although the thermodynamics must apply to the entire system it may nevertheless be appropriate to consider as the canonical ensemble a host of those regions where the internal back stresses are the highest providing all regions are in thermal contact and the internal stress fields remain constant.

2. As shown by Hirth and Nix the atomic displacements at fixed distant strain centers during the small activation motion of a dislocation do not introduce additional interaction energies. Consequently, only the local internal stress at the dislocation is significant to the free energy of activation.

3. On the other hand, the internal stresses in the region of activation must vary somewhat with the applied stress. For example, when constant strain-rate tests are conducted at lower temperatures the values for τ increase and therefore τ_A' might also increase due to changes in the more distant dislocation configurations. In this event τ_A' becomes a function of τ, in addition to being dependent on the cold-worked state. Over the athermal region τ_A' will decrease linearly and very slightly with temperature in parallel with the effect of temperature on the modulus of elasticity. But the linear extrapolation of τ_A' over the lower temperature thermally activated region is no longer wholly justified. Thus U should be formulated as $U \equiv U\{\tau, T\}$.

5. Limited current experimental evidence seems to suggest that τ_A is not very sensitive to τ (vide Fig. 8). Consequently in these instances it is not critical as to which set of independent variables (τ, T or τ^*, T) should be employed. More careful experimental investigations are now required to explore these issues.

6. Another feature that requires exploration at the same time is the possible variation of ρ_m with τ or τ^*. At present there is no satisfactory justification for making the assumption that ρ_m remains constant.

7. The above discussion on athermal stress levels was limited to cases where the athermal back stress arises exclusively from internal stress fields. The concept of superposition is obviously invalid when the athermal stress level arises from a balance between the forward and reverse frequencies of activation as discussed in Section VIII.

Acknowledgements

The authors wish to express their appreciation to the United States Atomic Energy Commission for their support of this investigation through the Inorganic Materials Research Division of the Lawrence Radiation Laboratory of the University of California, Berkeley. The authors also thank Mr. James E. Bird for his assistance in preparing this manuscript.

Table 1

ACTIVATION ENERGIES

	APPLIED FORCE F	REGION X	ENERGY U^+
CONDITION I	$0 \le \tau b^2 \ell < \tau_A' b^2 \ell$	$0 \le x \le \lambda/2$ $\lambda/2 \le x \le \lambda$	~ INFINITE $\alpha\Gamma b - \tau b^2 \ell - \tau_A' b^2 \ell$
CONDITION II	$\tau_A' b^2 \ell \le \tau b^2 \ell \le$ $\alpha\Gamma b - \tau_A' b^2 \ell$	$0 \le x \le \lambda/2$ $\lambda/2 \le x \le \lambda$	$\alpha\Gamma b - \tau b^2 \ell + \tau_A' b^2 \ell$ $\alpha\Gamma b - \tau b^2 \ell - \tau_A' b^2 \ell$
CONDITION III	$\alpha\Gamma b - \tau_A' b^2 \ell \le \tau b^2 \ell \le$ $\alpha\Gamma b + \tau_A' b^2 \ell$	$0 \le x \le \lambda/2$ $\lambda/2 \le x \le \lambda$	$\alpha\Gamma b - \tau b^2 \ell + \tau_A' b^2 \ell$ 0

XBL 6910-5717

REFERENCES

1. John E. Dorn; Dislocation Dynamics, McGraw-Hill, New York, (1968), pp. 27-55.

2. A. K. Mukherjee and J. E. Dorn; J. Inst. of Metals, 93, 1964-65, pp. 397-401.

3. A. K. Mukherjee and J. E. Dorn; Trans. Met. Soc. AIME, 230, 1964, pp. 1065-69.

4. A. K. Mukherjee, W. G. Ferguson, W. L. Barmore and J. E. Dorn; J. Appl. Phys., 37, 1966, pp. 3707-13.

5. A. K. Mukherjee, J. E. Bird and J. E. Dorn; Trans. ASM, 62, 1969, pp. 155=179.

6. J. Fisher; Acta Met., 2, 1954, p. 9.

7. P. Flinn; Phys. Rev., 104, 1956, p. 350.

8. F. C. Frank and W. T. Read; Phys. Rev., 79, 1950, p. 722.

9. G. Saada; Acta Met., 8, 1960, p. 841.

10. G. Saada; Acta Met., 9, 1969, p. 160.

11. P. Guyot; Acta Met., 14, 1966, p. 955.

12. G. Taylor; Proc. Roy. Soc., 145A, 1934, p. 362.

13. N. Mott; Phil. Mag., 43, 1952, p. 1151.

14. A. Seeger, J. Diehl, S. Mader and H. Rebstock; Phil. Mag., 2, 1957, p. 323.

15. J. D. Mote, K. Tanaka and J. E. Dorn; Trans. Met. Soc. AIME, 221, 1961, p. 858.

16. A. Seeger, S. Mader, H. Kronmüller; Electron Microscopy and Strength of Crystals, Interscience Publishers, New York, (1962), pp. 665-712.

17. A. Cottrell and B. Bilby; Proc. Phy. Soc., A62, 1964, p. 49.

18. N. Mott and F. R. N. Nabarro; Proc. Phys. Soc., 52, 1940, p. 84.

19. A. Cochardt, G. Schoeck and H. Wiedersich; Acta Met., 3, 1955, p.533.

20. R. Fleischer; Acta Met., 10, 1962, p. 835.

21. R. Fleischer and W. Hibbard; "The Relation Between the Structure and Mechanical Properties of Metals", Her Majesty's Stationery Office, London, 1963, p. 262.

22. J. Friedel; Dislocations, Pergamon Press, Oxford, 1964, p. 351.

23. A. R. Rosenfield, G. T. Hahn, A. L. Bement, Jr., and R. I. Jaffee, eds., Dislocation Dynamics, McGraw-Hill, New York, (1968), p. 29.

24. M. Fine: "The Relation Between the Structure and Mechanical Properties of Metals", Her Majesty's Stationery Office, London, 1963 p. 299.

25. J. Friedel; "Dislocations", Pergamon Press, Oxford, 1964, p. 376.

26. A. Seeger; Proc. 2nd U. N. Inter. Conf. PUAE, 6, 1968, p. 250.

27. J. Diehl and W. Shilling; Proc. 3rd U. N. Inter. Conf. PUAE, 9, 1964 p. 72.

28. J. Diehl, G. Seidel and L. Nieman; Phys. Stat. Sol., 11, 1965, p.339 Phys. Stat. Sol., 12, 1965, p. 405.

29. R. Peierls; Proc. Phys. Soc., 51- 1940, p. 34.

30. A. Seeger; Phil. Mag., 1, 1956, p. 651.

31. J. Friedel; "Electron Microscopy and Strength of Crystals", Interscience Publishers, 1963, p. 605.

32. V. Celli, M. Kabler, T. Nimoiya and R. Thomson; Phys. Rev., 131, 1963, p. 58.

33. J. Dorn and S. Rajnak; Trans. Met. Soc. AIME, 230, 1964, p. 1052.

34. P. Guyot and J. Dorn; Canad. J. of Phys., 45, 1967, p. 983.

35. J. E. Dorn and A. K. Mukherjee; Trans. Met. Soc. AIME, 245, 1969, p. 1493.

36. A. Cottrell; Phil. Mag., 43, 1952, p. 645.

37. A. Seeger; Phil. Mag., 45, 1954, p. 771.

38. J. Friedel; "Dislocations", Pergamon Press, Oxford, 1964, p. 264.

39. C. Zener; "Elasticity and Anelasticity of Metals", Univ. of Chicago Press, 1958, p. 89.

40. J. Eshelby; Proc. Roy. Soc., A197, 1949, p. 396.

41. A. Granato and K. Lucke; J. Appl. Phys., 27, 1956, p. 789.

42. G. Liebfried; Z. Physik, 127, 1950, p. 344.

43. W. Mason; Phys. Rev., 97, 1955, p. 557.

44. W. Mason; Phys. Rev., 143, 1966, p. 339.

45. A. Akheiser; J. Phys. USSR, 1, 1939, p. 277.

46. W. Mason; J. Acons. Soc. Amer., 32, 1960, p. 458.

47. W. Mason and T. Bateman; J. Acons. Soc. Amer., 36, 1964, p. 644.

48. W. Mason; J. Appl. Phys., 35, 1964, p. 2779.

49. U. Kocks; Phil. Mag., 13, 1966, p. 541.

50. T. Stefansky and J. E. Dorn; "The Role of Dislocation Flexibility in the Strengthening of Metals", UCRL Report No. 18405 Rev., April 1969 Univ. of California, Berkeley, California, Trans. AIME, 245, 1869 (1969).

51. A. Foreman and M. Makin; Phil. Mag., 14, 1966, p. 911.

52. J. Friedel; "Dislocations", Pergamon Press, Oxford, 1964, p. 224.

53. N. F. Mott and F. R. N. Nabarro; Proc. Phys. Soc., 52, 1940, p. 86.

54. F. R. N. Nabarro; Proc. Phys. Soc., 58, 1949, p. 669.

55. A. H. Cottrell; "Dislocations and Plastic Flow in Crystals", Oxford, 1958.

56. H. Gleiter; Acta Met., 16, 1968, p. 829.

57. V. Gerold; Acta Met., 16, 1968, p. 823.

58. J. Friedel; "Dislocations", Addison-Wesley Pub. Co., 1964, p. 351.

59. W. Frank; Phys. Stat. Solids, 26, 1968, p. 197.

60. S. K. Mitra and J. E. Dorn; Trans. Met. Soc. AIME, 224, 1962, p.1062

61. K. R. Evans and W. F. Flanagan; Phil. Mag., 16, 1968, p. 535.

62. J. C. M. Li; Canad. J. Phys., 45, 1967, p. 493.

63. J. C. M. Li; "Dislocation Dynamics", McGraw-Hill Co., New York, 1968 p. 87.

64. H. S. Chen, J. J. Gilman and A. K. Head; J. A. P., 35, 1964, p. 2502.

65. A. H. Cottrell and R. J. Stokes; Proc. Roy. Soc., A233, 1955, p. 17.

66. K. Ono and A. W. Sommer; Technical Report No. 3, Office of Naval Research, Contract N 00014-C-67-0439, May 1969.

67. Y. Nakada and A. S. Keh; Acta Met., 16, 1968, p. 903.

68. S. Glasstone, K. J. Laidler and H. Eyring; "The Theory of Rate Processes", McGraw-Hill Co., New York, (1941).

69. G. Schoeck, Phys. Stat. Sol., 8, 1965, p. 499.

70. J. P. Hirth and W. D. Nix; "An Analysis of the Thermodynamics of Dislocation Glide", Rept. No. SU-DMS-69-R-45, Dept. of Matls. Sci., Stanford Univ., 1969.

71. C. Wert and C. Zener; Phys. Rev., 76, 1949, p. 1169.

72. G. H. Vineyard; J. Phys. Chem. Solids, 3, 1957, p. 121.

73. A. V. Granato, K. Lucke, J. Schliff and L. J. Teutonico; J. Appl. Phys., 33, 1964, 2732.

74. J. C. M. Li; "Dislocation Dynamics", McGraw-Hill Co., New York, 1968 p. 87.

75. Z. S. Basinski; Acta Met., 5, 1957, p. 684, Phil. Mag. 4, 1959, p.393

76. G. Gibbs; Phys. Stat. Sol., 5, 1964, p. 693, Phys. Stat. Sol., 5, 1964, K125, Phys. Stat. Sol., 10, 1965, p. 507.

Appendix I: Symbols

A	= Average area swept out by dislocation per successful event
A'	= Constant
b	= Burger's vector
c	= Atom fraction of solute
D	= Diffusivity
f^*	= Helmholtz free energy of activation
G	= Shear modulus of elasticity
h	= Planck's constant
h'	= distance moved per activation
k	= Boltzmann constant
$l = 2L$	= Dislocation segment length
L_c	= Critical length of L
l_s	= Distance between obstacles in a square array
m	= Number of degrees of vibrational freedom that change during activation
N	= Number of sites for thermal activation per unit volume
N_a^*/N_a	= Equilibrium fraction of activated atoms per atom in the initial state
n	= A constant (1∿7)
T	= Temperature in °K
T_c	= Critical temperature
T_m	= Melting point in °K
U	= Isothermal work of activation
U_n	= Isothermal work to nucleate a pair of kinks in the forward direction
U_{nb}	= Isothermal work required to nucleate a pair of kinks in the backward direction
U_k	= Energy of a kink

v	= Velocity of dislocations
$\bar{v}$	= Average velocity of dislocations
$\bar{v}'$	= Average translational velocity of an atom
v_D	= Velocity of dislocation under the action of damping
Z^*_{1t}	= Translational partition function for activate state
Z_{1v}, Z_{2v}, Z_{3c}	= Vibrational partition functions for the initial state
Z^*_{2v}, Z^*_{3v}	= Vibrational partition function for the activated state
α	= Constant, to represent the maximum obstacle force as $\alpha\,\Gamma$
β	= Constant
δ	= Distance along reaction coordinate in the activated state
ε^*	= Energy difference between the activated and ground state, i.e. activation energy
$\dot{\gamma}$	= Strain rate
Γ	= Dislocation line energy $Gb^2/_2$
ν_1, ν_2, ν_3 etc.	= Vibrational frequency for initial state
ν^*_2, ν^*_3 etc.	= Vibrational frequencies for the activated state
ν_A	= Net frequency of activation
ν'	= Attempt frequency
ν_o	= Debye frequency
ν_i	= Atomic vibrational frequencies
λ	= Wave length of internal back stress
ρ	= Dislocation density
ρ_m	= Mobile dislocation density
τ	= Applied shear stress
τ_A	= Athermal stress
τ'_A	= Amplitude of internal back stress
τ^*	= Effective stress = $\tau-\tau_A$

τ_i = Internal stress

τ_p = Peierls stress

τ_s = Athermal stress due to disordering of short-range ordered alloys

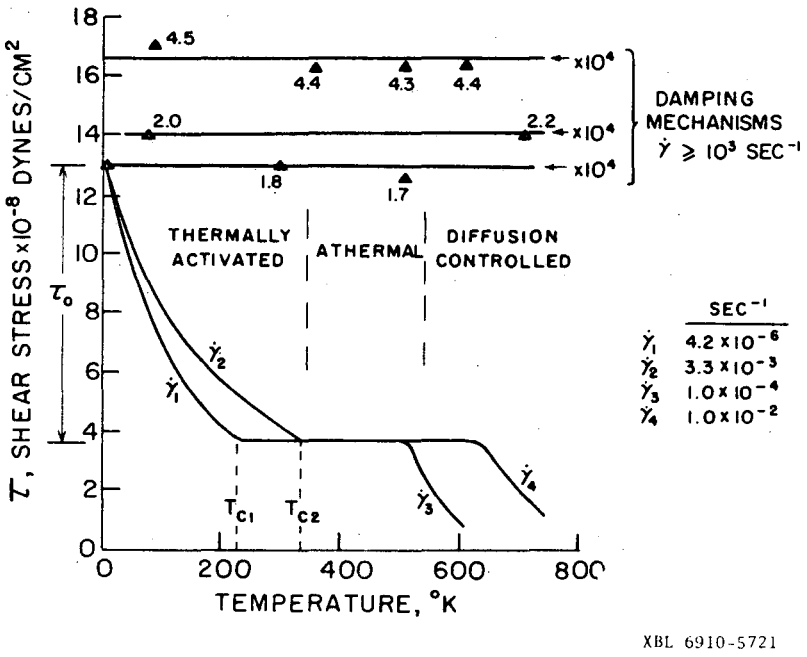

Fig. 1 Flow Stress-Temperature-Strain Rate relationships for single crystals of AgMg.

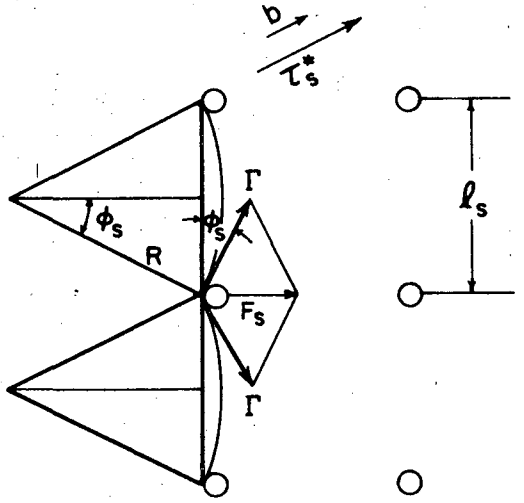

$$\tau_s^* = \frac{\Gamma}{bR} \qquad (4)$$

$$F_s = 2\Gamma \sin \phi_s = \frac{2\Gamma \ell_s}{2R} = \tau_s^* b \ell_s \qquad (5)$$

(a)

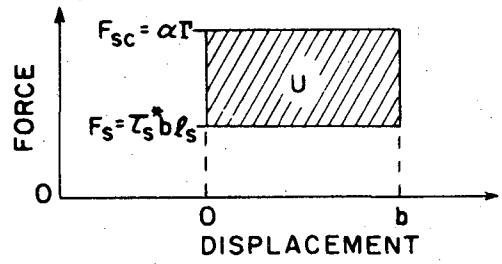

$$U^+ = \alpha\Gamma b - \tau_s^* b \ell_s b \qquad (6)$$

$$U^- = \alpha\Gamma b + \tau_s^* b \ell_s^2 \qquad (7)$$

(b)

XBL 6910-5718

Fig. 2 Prototype for cutting of "square" array of localized obstacles.

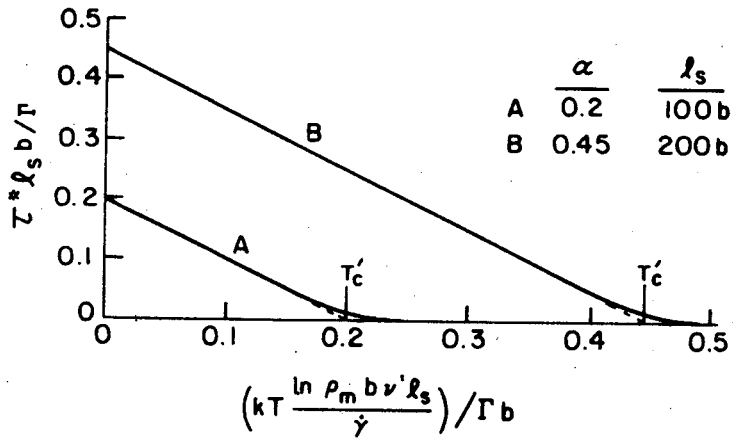

Fig. 3. Flow stress versus temperature relationship for cutting of square array (in dimensionless units).

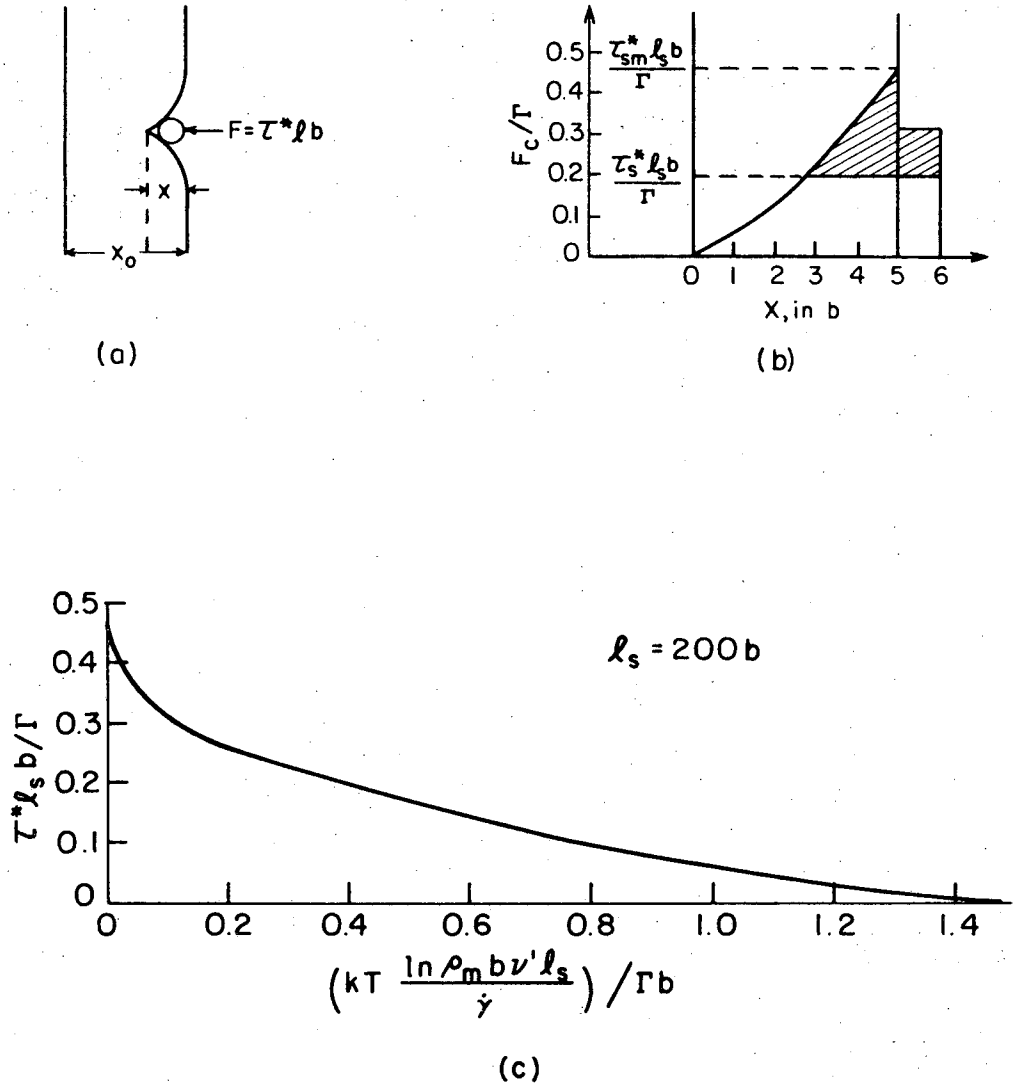

Fig. 4 Cutting of non-reactive forest dislocations by dissociated glide dislocations.
a) Partially formed constriction.
b) Force-displacement diagram.
c) Flow stress versus temperature in dimensionless units (l_s = 200b).

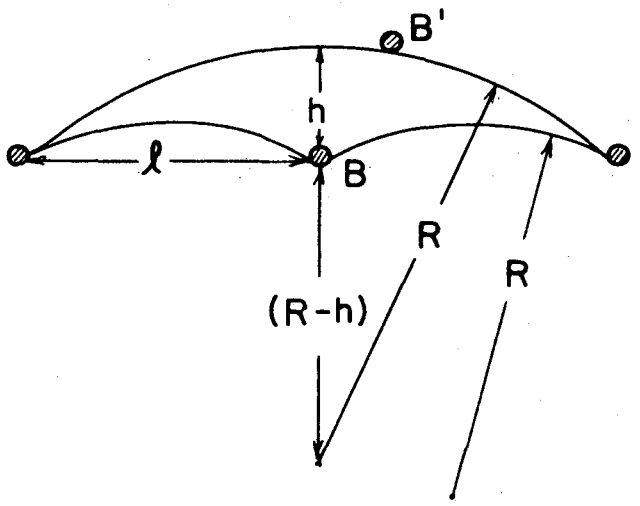

$$\ell h = \ell_s^2$$

$$\ell^2 = 2Rh - h^2$$

FOR $h \ll 2R$

$$\ell^2 \simeq 2R\ell_s^2/\ell \qquad (10)$$

$$\ell \simeq (2R\ell_s^2)^{1/3} = \left(\frac{2\Gamma\ell_s^2}{\tau^* b}\right)^{1/3}$$

XBL 6910-5723

Fig. 5 Geometry of randomly distributed localized obstacles.

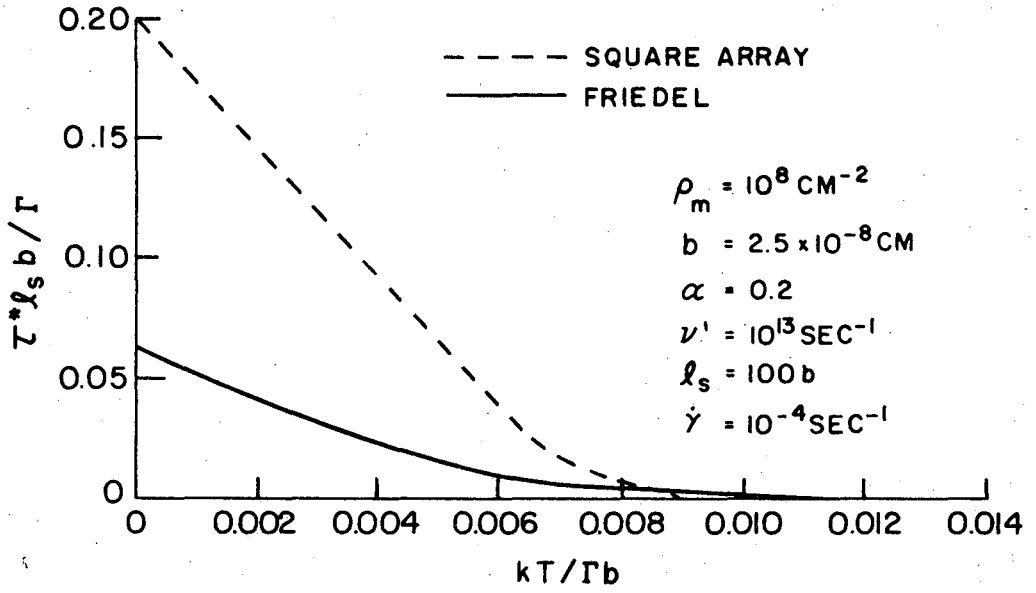

XBL 6910-5728

Fig. 6 Comparison of predictions based on Friedel's model with those for a square array.

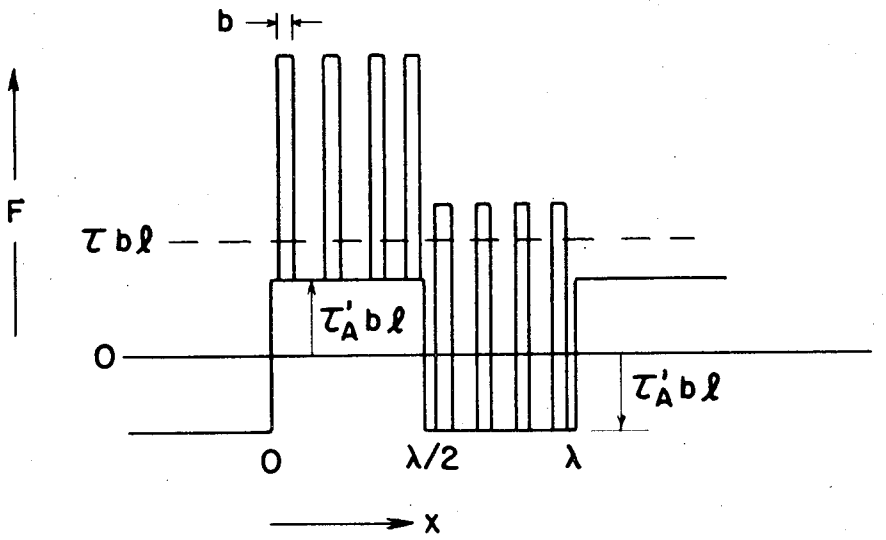

XBL 6910-5725

Fig. 7 Schematic representation of the internal back stresses as a slip function of wave length λ.

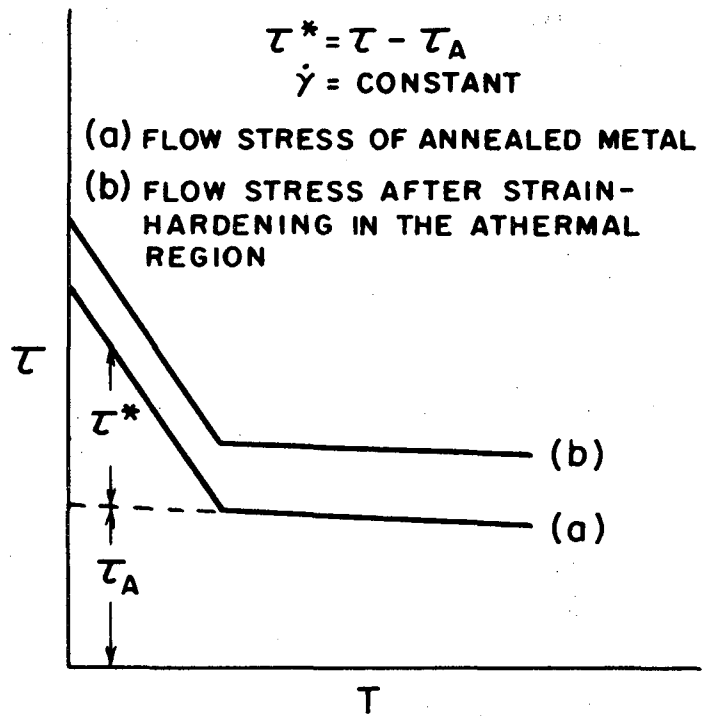

XBL 6910-5706

Fig. 8 τ - T relationship for case where short-range barriers are uneffected by strain hardening.

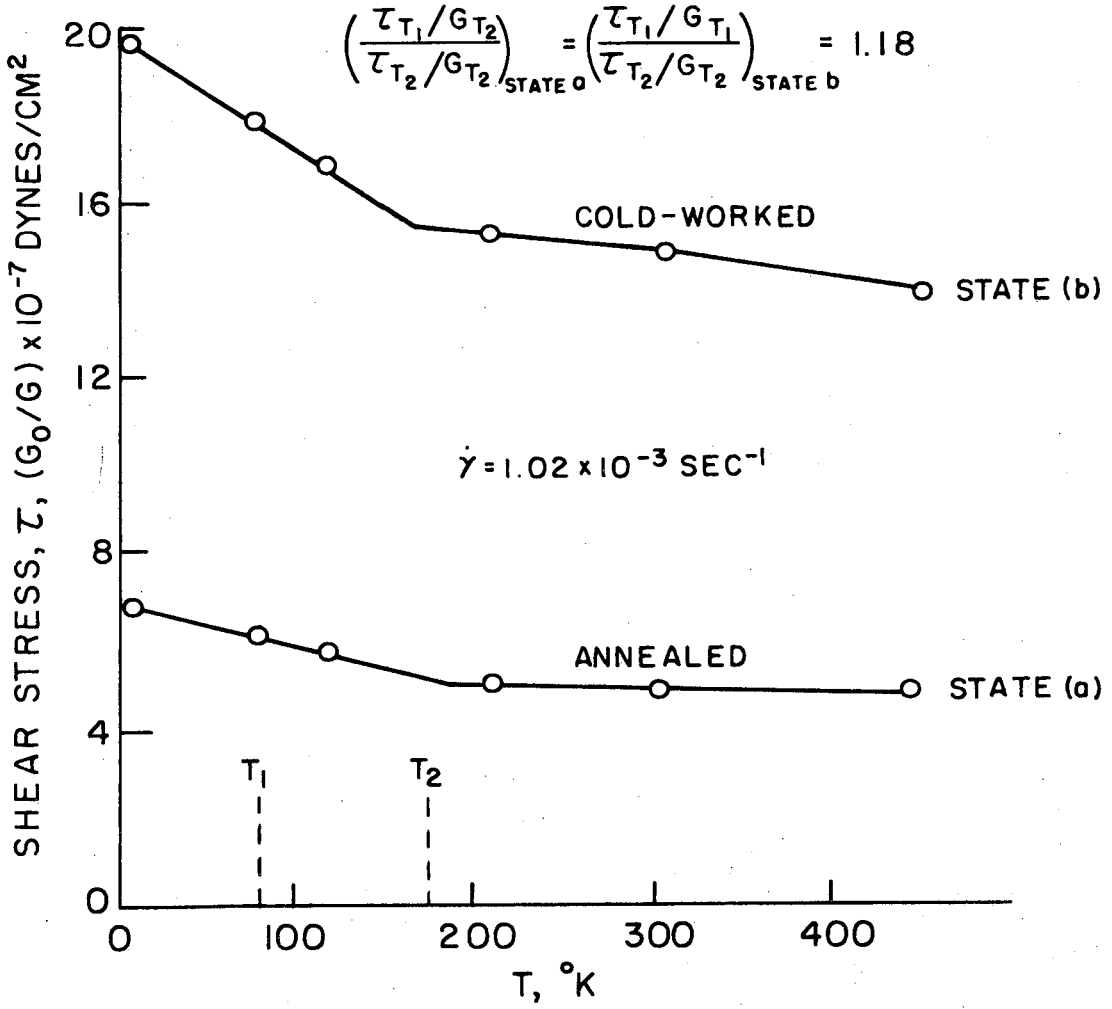

FIG. 9 COTTRELL STOKES RATIO IN F.C.C. ALUMINUM.

XBL 6910-5722

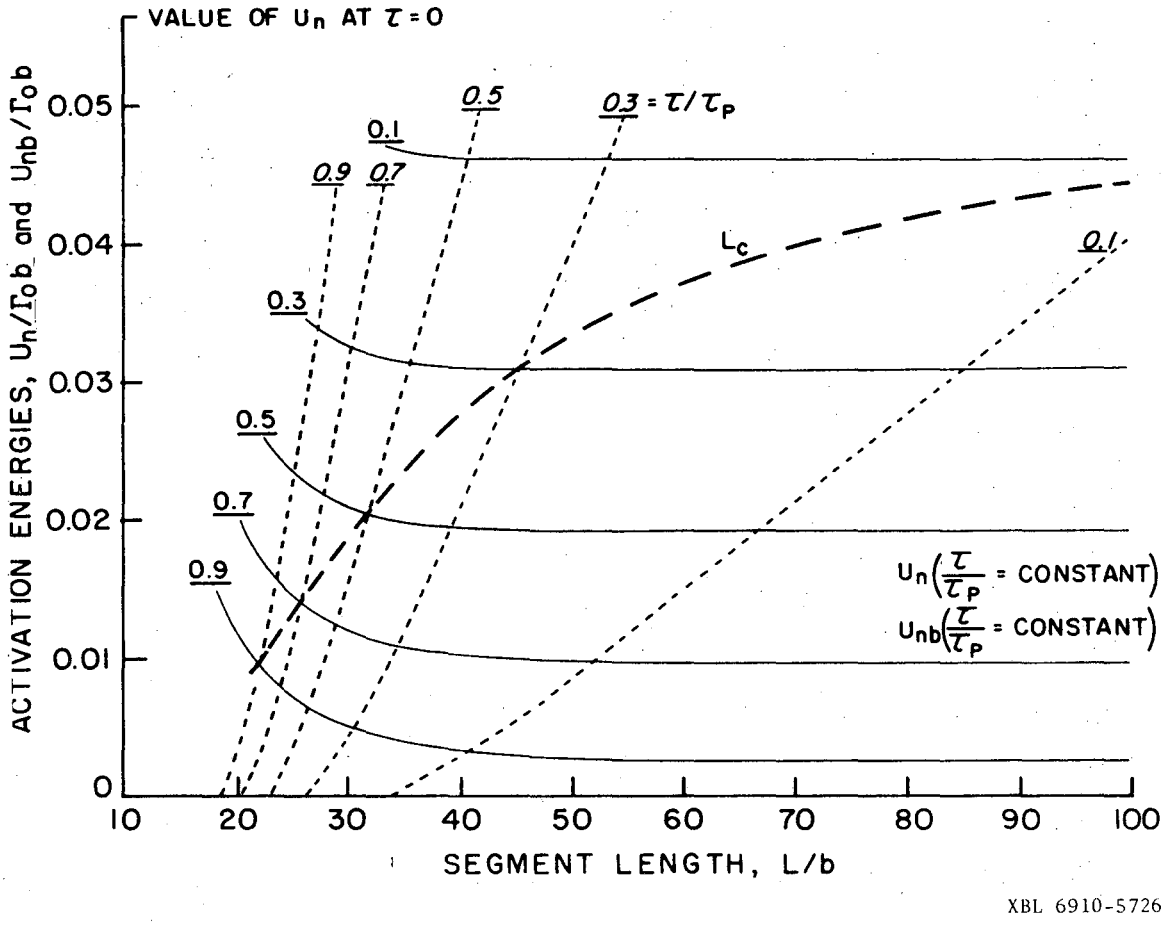

Fig. 10 Effect of segment length on U_n (solid line) and U_{nb} (dotted line).

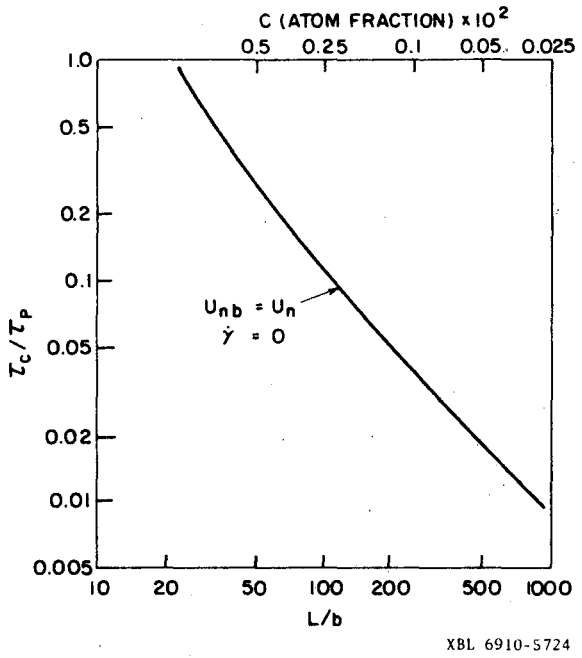

Fig. 11. Critical applied stress vs segment length for case $U_n = U_{nb}$.

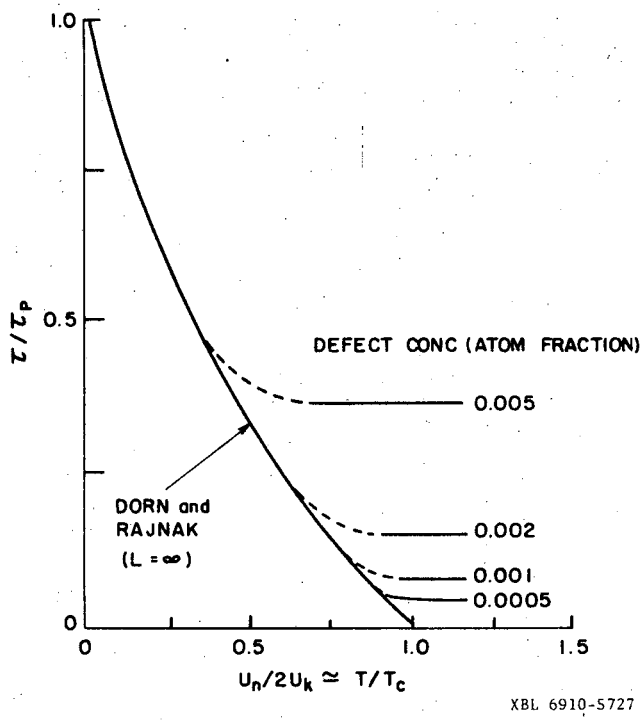

Fig. 12. Theoretically predicted τ - T relationship for nucleation limited double kink process (after Ono and Sommers, ref. 66).

LEGAL NOTICE

TECHNICAL INFORMATION DIVISION
LAWRENCE RADIATION LABORATORY
UNIVERSITY OF CALIFORNIA
BERKELEY, CALIFORNIA 94720